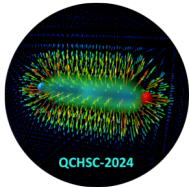


# Polyakov loop, QCD thermodynamics and observables

Yi Lu

Peking University

XVIth Quark Confinement and the Hadron Spectrum



Cairns, Aug 22, 2024

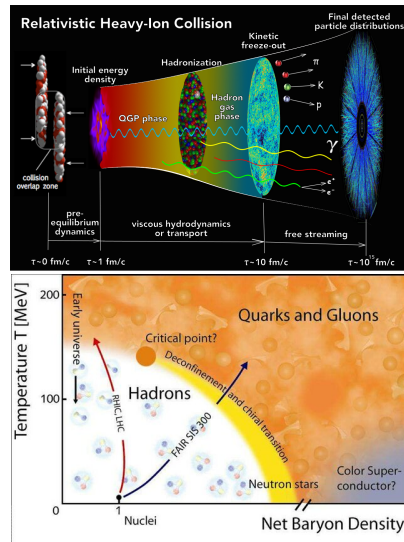


# Introduction

- **Thermodynamics** of QCD – quark-gluon matter in heavy-ion collisions, evolution of the early Universe, the origin of visible mass, etc.
- QCD phase structure – continuous efforts from first-principles calculations; running and planned experiment at RHIC-STAR, FAIR-GSI, NICA, HIAF...
- **Observables** to connect theory and experiment – particle yields, fluctuations, polarisation, (collective) flows, jets, ...

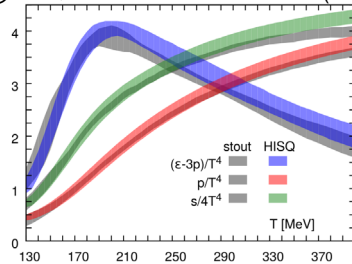
*The Present and Future of QCD*, QCD Town Meeting  
White Paper, 2023.

G. Aarts, J. Phys. Conf. Ser. 706: 022004 (2016)

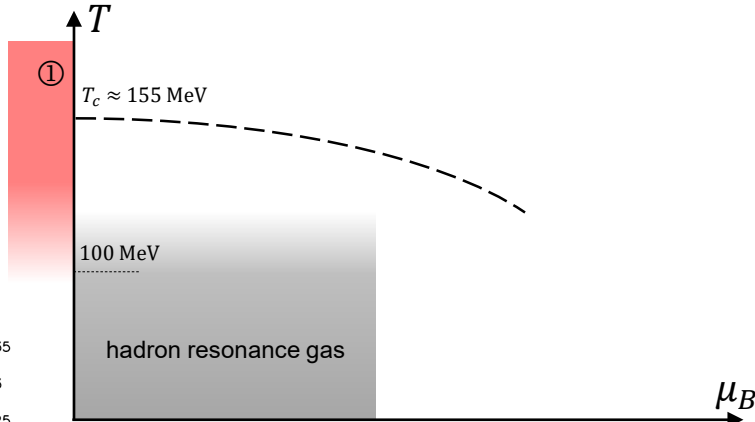
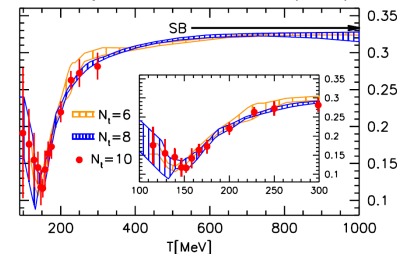


# QCD equation of state (EoS)

① hotQCD Collab. PRD 90: 094503 (2014)



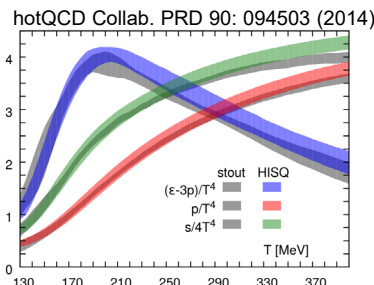
Borsanyi et al. JHEP 11, 077 (2010)



QCD pressure; at zero  $\mu_B$ :

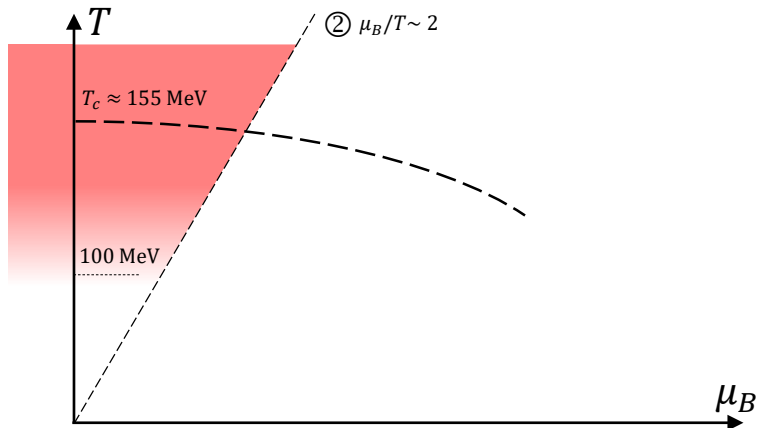
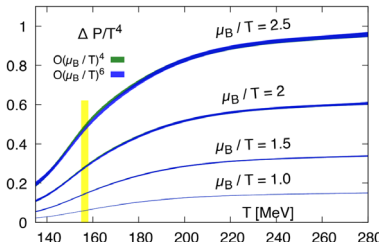
$$P(T, 0)$$

# QCD equation of state (EoS)



② Taylor expansion, e.g.:

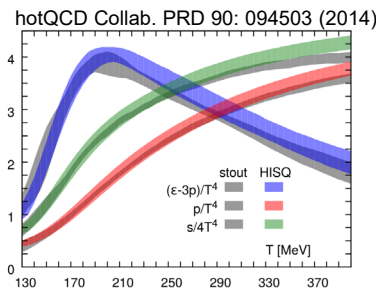
hotQCD Collab. PRD 105: 074511 (2022)



finite  $\hat{\mu}_B = \mu_B/T$ :

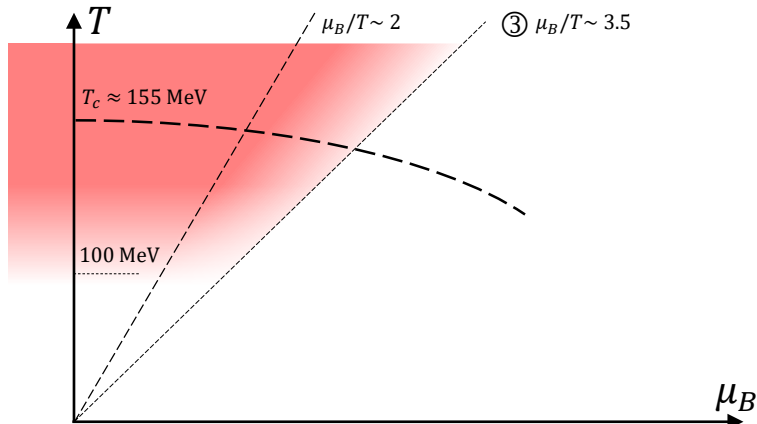
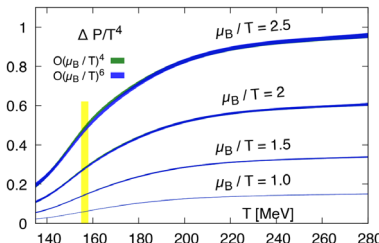
$$P(T, \hat{\mu}_B) = P(T, 0) + \frac{c_2(T)}{2!} \hat{\mu}_B^2 + \frac{c_4(T)}{4!} \hat{\mu}_B^4 + \dots$$

# QCD equation of state (EoS)



**Taylor expansion, e.g.:**

hotQCD Collab. PRD 105: 074511 (2022)

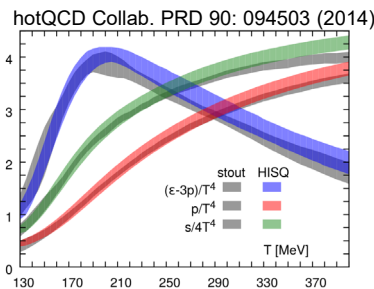


③ **T' expansion:** Borsanyi et al. (WB Collab.) PRL 126: 232001 (2021)  
**Pade:** hotQCD Collab. PRD 105: 074511 (2022)

$$P(T, \hat{\mu}_B) = P(T, 0) + \Delta P(T, \hat{\mu}_B)$$

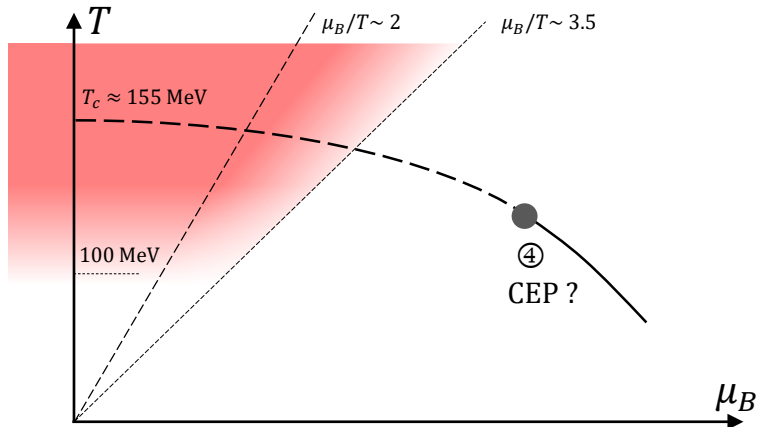
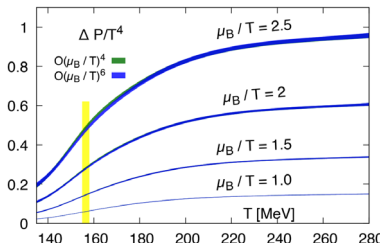
methods with improved converges radius.

# QCD equation of state (EoS)



**Taylor expansion, e.g.:**

hotQCD Collab. PRD 105: 074511 (2022)



**T' expansion:** Borsanyi et al. (WB Collab.) PRL 126: 232001 (2021)

**Pade:** hotQCD Collab. PRD 105: 074511 (2022)

- ④ **Estimated CEP still afar at  $\mu_B \sim 600$  MeV:** (see also in F. Rennecke's talk)  
discrete (lattice) - Clarke et al., 2405.10196, and continuum (functional QCD)  
– Fu et al, PRD (2019), Gao et al., PLB (2020), Gunkel et al. PRD (2021)

## Thermodynamics at finite temperature and density

$$P(T, \mu_B) = P(T, 0) + \int_0^{\mu_B} n_B(T, \mu) d\mu, \quad n_B = \frac{1}{3}(n_u + n_d + n_s + \dots).$$

General thermodynamics:  $n_q = \langle \bar{q} \gamma_4 q \rangle = -T \sum_{\omega_p} \int \frac{d^3 \mathbf{p}}{(2\pi)^3} \text{tr}_{C,D} [\gamma_4 G_q(\tilde{p})].$

Quark propagator in nonperturbative QCD ( $\tilde{p} = (\mathbf{p}, \omega_p + i\mu_q)$ ):

$$G_q^{-1}(\tilde{p}) = i(\omega_p + i\mu_q + gA_4)\gamma_4 Z_q^E(\tilde{p}^2) + i\gamma \cdot \mathbf{p} Z_q^M(\tilde{p}^2) + Z_q^E M_q(\tilde{p}^2),$$

universal in both discrete and continuum approaches.

# Thermodynamics at finite temperature and density

$$P(T, \mu_B) = P(T, 0) + \int_0^{\mu_B} n_B(T, \mu) d\mu, \quad n_B = \frac{1}{3}(n_u + n_d + n_s + \dots).$$

General thermodynamics:  $n_q = \langle \bar{q} \gamma_4 q \rangle = -T \sum_{\omega_p} \int \frac{d^3 \mathbf{p}}{(2\pi)^3} \text{tr}_{C,D} [\gamma_4 G_q(\tilde{p})].$

Quark propagator in nonperturbative QCD ( $\tilde{p} = (\mathbf{p}, \omega_p + i\mu_q)$ ):

$$G_q^{-1}(\tilde{p}) = i(\omega_p + i\mu_q + gA_4)\gamma_4 Z_q^E(\tilde{p}^2) + i\gamma \cdot \mathbf{p} Z_q^M(\tilde{p}^2) + Z_q^E M_q(\tilde{p}^2),$$

universal in both discrete and continuum approaches.

- chiral phase transition: quark dynamical mass  $M_q(\tilde{p}^2)$  (essentially  $\langle \bar{q}q \rangle$ );
- confinement - deconfinement:  $A_4$ , i.e. the **Polyakov loop**:

$$\mathcal{L}[A_4] = \frac{1}{N_c} \text{tr } \mathcal{P} \exp \left( ig \int_0^\beta dx_4 A_4 \right).$$

## I. Phenomenological method

- combine with phase transition studies

YL, F. Gao, B. C. Fu, H. C. Song, Y. X. Liu, Phys. Rev. D 109: 114031 (2024).

Consider the nonperturbative regime of the momentum:

$$Z_q^{E,M}(\tilde{p}^2) = Z_q^{(0)} + \mathcal{O}(\tilde{p}^2), \quad M_q(\tilde{p}^2) = M_q^{(0)} + \mathcal{O}(\tilde{p}^2),$$

the leading contribution suggests a phenomenological construction of  $G_q$  in terms of  $O_X$ :

$$O_\chi = M_q^{(0)}, \quad O_A = \mathcal{L},$$

$$\left[ G_q^{(0)}(\tilde{p}) \right]^{-1} = Z_q^{(0)} \left( i(\omega_p + i\mu_q + gA_4[O_A])\gamma_4 + i\gamma \cdot \mathbf{p} + M_q^{(0)}[O_\chi] \right);$$

Consider the nonperturbative regime of the momentum:

$$Z_q^{E,M}(\tilde{p}^2) = Z_q^{(0)} + \mathcal{O}(\tilde{p}^2), \quad M_q(\tilde{p}^2) = M_q^{(0)} + \mathcal{O}(\tilde{p}^2),$$

the leading contribution suggests a phenomenological construction of  $G_q$  in terms of  $O_X$ :

$$O_\chi = M_q^{(0)}, \quad O_A = \mathcal{L},$$
$$\left[ G_q^{(0)}(\tilde{p}) \right]^{-1} = Z_q^{(0)} \left( i(\omega_p + i\mu_q + gA_4[O_A])\gamma_4 + i\gamma \cdot \mathbf{p} + M_q^{(0)}[O_\chi] \right);$$

With frequency-independent  $M_q^{(0)}$ , the (renormalised) thermodynamic quantities become analytic functions in terms of the order parameters, e.g.:

$$n_q(T, \mu_q) = 2N_c T \int \frac{d^3 \mathbf{p}}{(2\pi)^3} f_q(M_q^0, \mathcal{L}, \mathcal{L}^\dagger; \mathbf{p}, T, \mu_q).$$

Knowledge on the phase structure  $\rightarrow$  thermodynamics.

## Combine with phase transition studies - $M_q$

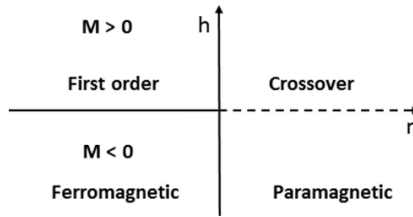
Phenomenology around CEP is captured by  
3D Ising parametrisation -  $Z(2)$ <sup>1,2</sup>:

$$\mathcal{M}_{\text{Ising}} = \mathcal{M}_0 R^\beta \theta,$$

$$h = h_0 R^{\beta\delta} \theta (1 + a\theta^2 + b\theta^4),$$

$$r = R(1 - \theta^2).$$

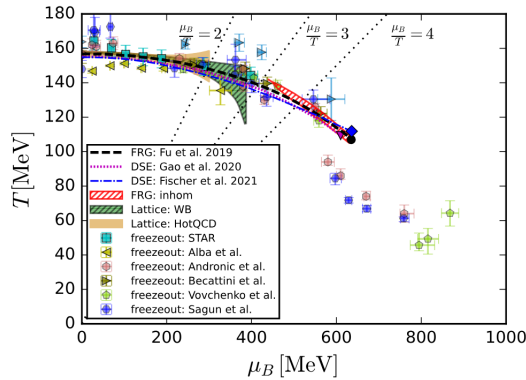
Map  $\mathcal{M}_{\text{Ising}} \in (-1, 1)$  to  $M_q^{(0)} \in (M_q^{\text{vac.}}, 0)$ : linear.



<sup>1</sup> Parotto et.al. PRC 101: 034901 (2020).

<sup>2</sup> Kahangirwe et.al. PRD 109: 094046 (2024).

Modified (non-linear) map  $(r, h) \leftarrow (T, \mu_B)$ :  
constrained by the up-to-date phase transition  
line:  $T_c/T_0 = 1 - \kappa_2 (\mu_B/T_0)^2 + \kappa_4 (\mu_B/T_0)^4 + \dots$ .  
(Plot: Fu, Commun. Theor. Phys. 74: 097304 (2022).)



## Combine with phase transition studies - $M_q$

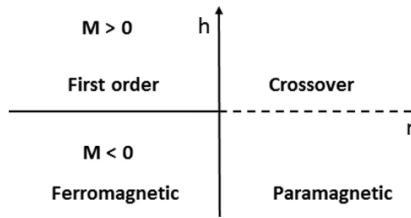
Phenomenology around CEP is captured by  
3D Ising parametrisation -  $Z(2)$ <sup>1,2</sup>:

$$\mathcal{M}_{\text{Ising}} = \mathcal{M}_0 R^\beta \theta,$$

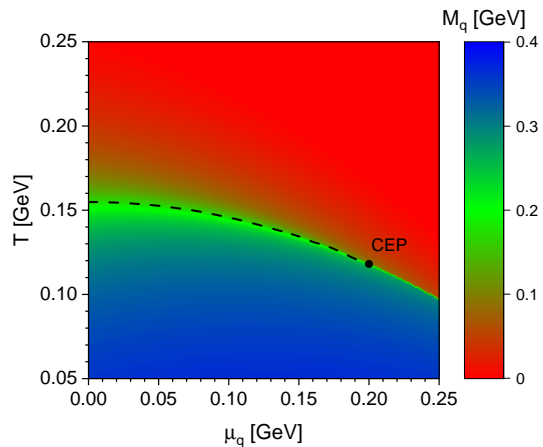
$$h = h_0 R^{\beta\delta} \theta (1 + a\theta^2 + b\theta^4),$$

$$r = R(1 - \theta^2).$$

Map  $\mathcal{M}_{\text{Ising}} \in (-1, 1)$  to  $M_q^{(0)} \in (M_q^{\text{vac.}}, 0)$ : linear.



Modified (non-linear) map  $(r, h) \leftarrow (T, \mu_B)$ :  
constrained by the up-to-date chiral phase  
transition line.



<sup>1</sup> Parotto et.al. PRC 101: 034901 (2020).

<sup>2</sup> Kahangirwe et.al. PRD 109: 094046 (2024).

## Combine with phase transition studies - $\mathcal{L}$

Not all crystal clear, especially at finite density... preliminary study from known inputs.

Zero  $\mu_B$ : data taken from functional RG study <sup>1</sup>.

Finite  $\mu_B$ :  $T'$  parametrisation <sup>2</sup>

$$T'/T_0 = T/T_0 + \kappa_2(\mu_B/T_0)^2,$$

$$\mathcal{L}(T, \mu_B) = \mathcal{L}^\dagger(T, \mu_B) = \mathcal{L}(T', 0);$$

$\kappa_2$ : close connection between the chiral and deconfinement phase transition (see e.g. <sup>3</sup>);

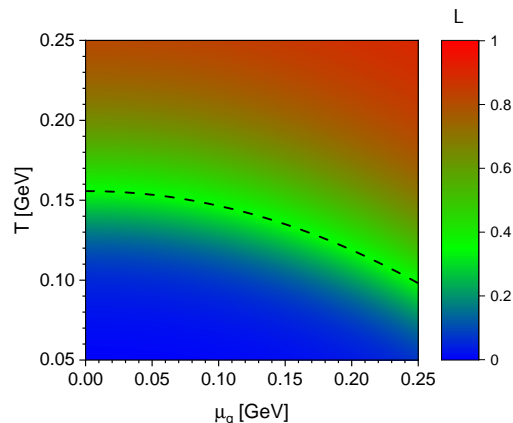
consequence of taking  $\mathcal{L} \simeq \mathcal{L}^\dagger$  is reflected in <sup>4</sup>.

<sup>1</sup> Fu and Pawłowski, PRD 92: 116006 (2015).

<sup>2</sup> Borsanyi et.al. (WB Collab.), PRL 126: 232001 (2021).

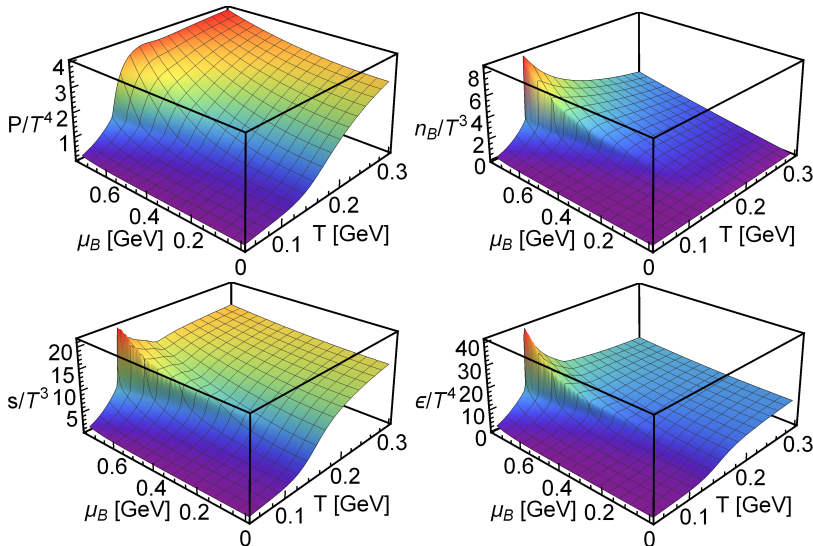
<sup>3</sup> Fischer et al., PRD 90: 034022 (2014).

<sup>4</sup> Fu et al., PRD 101: 054032 (2020).



# 2+1-flavor QCD EoS from the order parameters

Github: [EoS-PhaseDiagramMap](#)

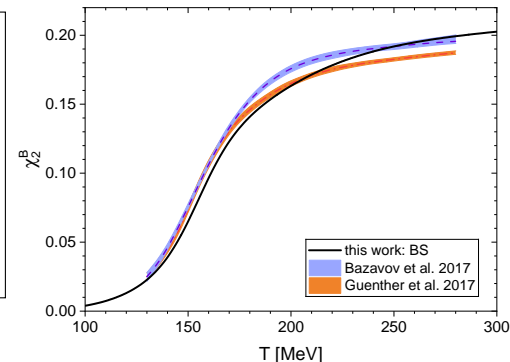
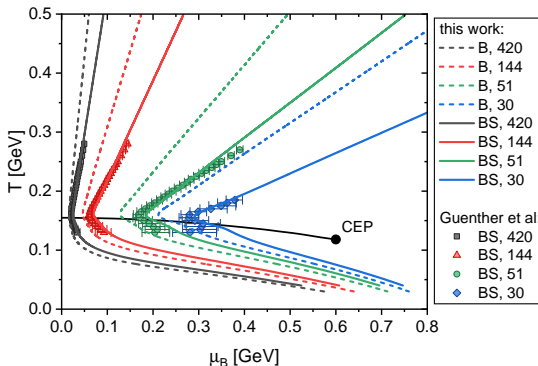


## 2+1-flavor QCD EoS from the order parameters

Isentropic trajectories:  $s/n_B = \text{const.}$ , compare with lattice QCD (left);  
compare with hadron resonance gas (HRG) model at low  $T$ : Zheng et al., 2407.03795.

Baryon number fluctuations:  $\chi_k^B = \frac{\partial^k(P/T^4)}{\partial(\mu_B/T)^k} = \frac{\partial^{k-1}(n_B/T^3)}{\partial(\mu_B/T)^{k-1}}$ ,

provides quantitative check for the limitations:  $\partial_T^i \partial_{\mu_B}^j P$  up to  $i + j \leq 2$ .

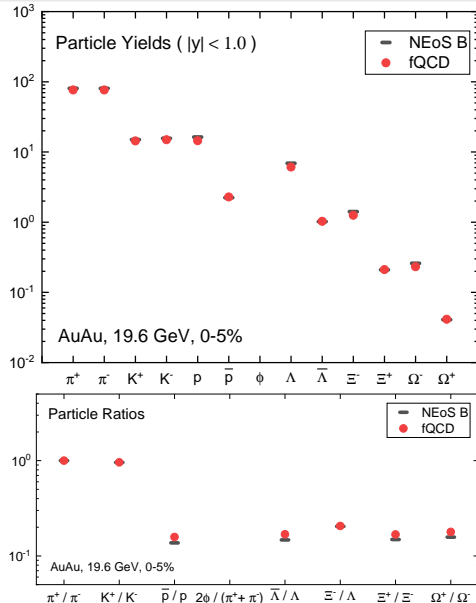


## II. Impacts of Polyakov loop on the observables in quark-gluon matter

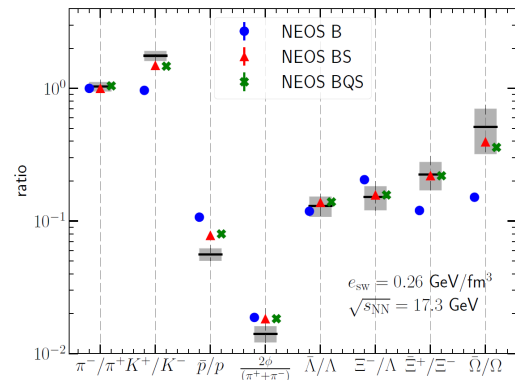
**YL**, F. Gao, B. C. Fu, H. C. Song, Y. X. Liu, Phys. Rev. D 109: 114031 (2024).

F. Gao, J. Harz, C. Hati, **YL**, I. Oldengott and G. White, 2309.00672 and 2407.17549.

# Impacts on heavy-ion collision



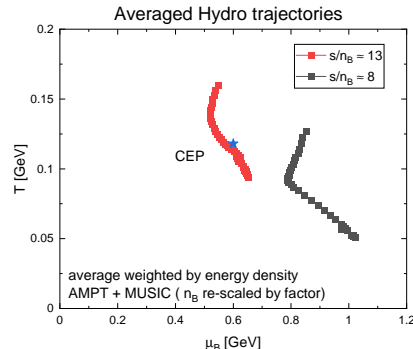
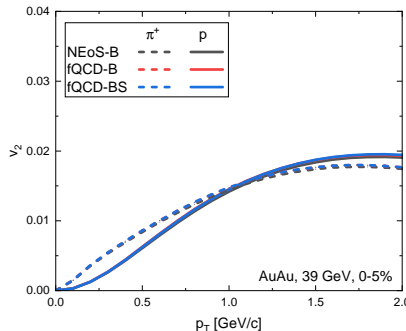
fQCD-based EoS as input of hydrodynamic simulation - viscous hydro. (MUSIC).  
Compare with NEoS<sup>1</sup> (HRG + lattice QCD) and experiment; right plot from<sup>1</sup>.



<sup>1</sup> Monnai et al., Phys. Rev. C 100, 024907 (2019).

# Impacts on heavy-ion collision

More on the elliptic flow  $v_2$  and dynamical evolution - ideal hydro. preliminary.  
A glimpse of 1st-order phase transition - with AMPT initial profile at 7.7 GeV.



Going beyond CEP and towards even higher density: need to separate  $L$  and  $L^\dagger$ .

# Impacts on cosmological phase transition

Lepton (flavour) asymmetries ( $Y_L$ ) and cosmological evolution:

$$Y_{L_\alpha} = \frac{n_{L_\alpha}}{s} = \frac{n_\alpha + n_{\nu_\alpha}}{s}, \quad \alpha = e, \mu, \tau,$$

$$Y_B = \frac{n_B}{s} = \sum_i \frac{b_i n_i}{s},$$

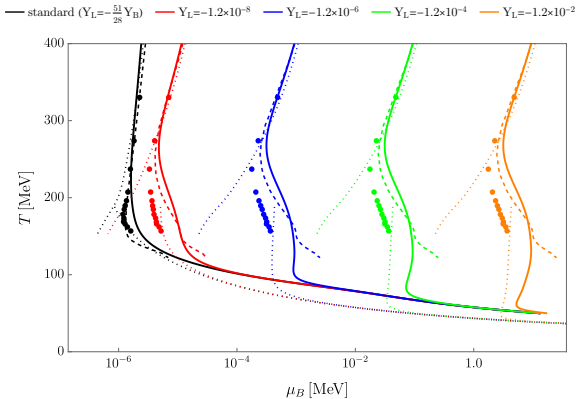
$$Y_Q = \frac{n_Q}{s} = 0 \quad \Leftrightarrow \quad n_Q = \sum_i q_i n_i = 0.$$

Further applications on the cosmological gravitational wave signal ( $\mathcal{O}(10^{-6})$  Hz):

Gao et al., 2309.00672 and 2407.17549.

Zheng et al., 2407.03795.

Impacts of Polyakov loop on the trajectories:  
solid: with  $\mathcal{L}$ ; dashed: w/o.  $\mathcal{L}$ ; dotted: HRG;



### III. Polyakov loop and glue dynamics

- YL, F. Gao, Y. X. Liu and J. Pawłowski, Phys. Rev. D 110, 014036 (2024)  
YL, F. Gao, Y. X. Liu and J. Pawłowski, in preparation.

The nonperturbative quark propagator:

$$G_q^{-1}(\tilde{p}) = i(\omega_p + i\mu_q + gA_4)\gamma_4 Z_q^E(\tilde{p}^2) + i\gamma \cdot \mathbf{p} Z_q^M(\tilde{p}^2) + Z_q^E M_q(\tilde{p}^2),$$

$A_4$  is essentially the gluon 1-point function (background field); for SU(3):

$$A_4 = \frac{2\pi T}{g} (\varphi_3 \lambda_3 + \varphi_8 \lambda_8), \quad \mathcal{L} = \frac{1}{3} \left[ e^{-i\frac{2\pi\varphi_8}{\sqrt{3}}} + 2e^{i\pi\frac{\varphi_8}{\sqrt{3}}} \cos \pi\varphi_3 \right].$$

The eigenvalues  $\varphi_{3,8}$  correspond to the representations of gluons / quarks, e.g.:

$$\varphi_3 = \{\pm\varphi, \pm\varphi/2, \pm\varphi/2, 0, 0\}, \quad \text{adjoint rep.,}$$

$$\varphi_3 = \{\pm\varphi/2, 0\}, \quad \text{fundamental rep.}$$

$\varphi_8$  reflects the difference between the conjugated Polyakov loops  $\mathcal{L}$  and  $\mathcal{L}^\dagger$ ;

## Polyakov loop potential and glue dynamics

Polyakov loop potential  $V[A_4]$  is the effective glue potential in terms of background field  $A_4$ ; Dyson-Schwinger equation (DSE) for  $V'[A_4] = \delta V[A_4]/\delta A_4$ <sup>1,2</sup>:

$$\frac{\delta(\Gamma - S)}{\delta A_0} = \frac{1}{2} \text{---} \text{---} \text{---} \frac{1}{6} \text{---} +$$

Alternatively, within fRG approach<sup>3</sup>.

We apply DSE with one-loop truncation<sup>1</sup>:

$$V[A_4] = V_{\text{glue}}[A_4] + V_q[A_4],$$

$$V_{\text{glue}}[A_4] = \frac{1}{2} V_{\text{Weiss}}[A_4] + V_a[A_4] + V_c[A_4],$$

$V_a$ ,  $V_c$  and  $V_q$  determined by the propagators (the 2-point functions);

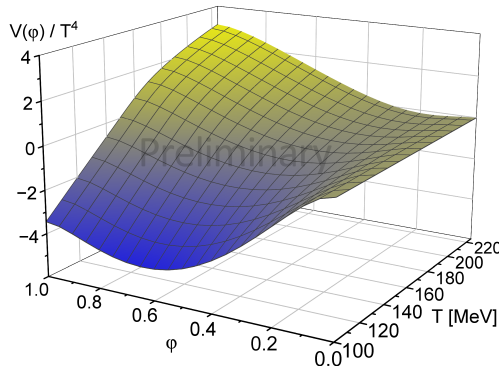
DSEs for the propagators - see G. Eichmann's talk; we refer to a recent DSE calculation<sup>4</sup>.

<sup>1</sup> Fischer et al., Phys. Lett. B 732: 273 (2014). <sup>2</sup> Fister and Pawłowski, Phys. Rev. D 88: 045010 (2013).

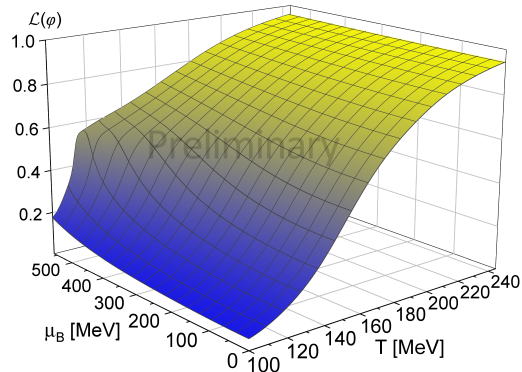
<sup>3</sup> Braun et al., Phys. Lett. B 684: 262 (2010). <sup>4</sup> YL, et al., Phys. Rev. D 110: 014036 (2024).

Preliminary study on the “center average”  $\varphi_8 \simeq 0$ , i.e.  $\mathcal{L} \simeq \mathcal{L}^\dagger$ .

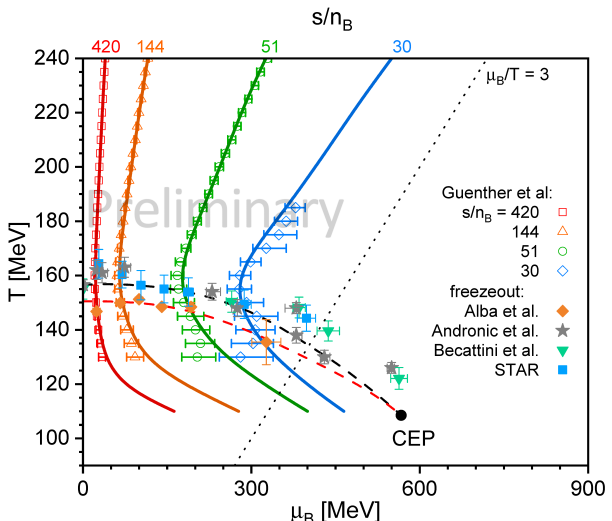
Full SU(3) potential at  $\mu_B = 0$   
as a function of  $\varphi_3$  and  $T$ :



Polyakov loop at finite  $(T, \mu_B)$ , and the deconfinement phase transition:



# Gluon background field and QCD thermodynamics



QCD isentropic trajectories via DSE:

$s/n_B = 420, 144, 51$  and  $30$  agree with lattice QCD<sup>2</sup>; meet with the freezeout points at  $\sqrt{s_{NN}} = 200, 62.4, 19.6$  and  $11.5$  GeV, respectively.

<sup>1</sup> Fischer et al., Phys. Lett. B 732: 273 (2014).

<sup>2</sup> Guenther et al (WB Collab.) Nucl. Phys. A 967: 720-723 (2017).

Progress on:

- Order parameter framework, as a functional-QCD-based model for EoS.
- Relevance of Polyakov loop on QCD thermodynamics in hadronic phase; impacts on particle yields and evolution trajectories.
- Probing glue dynamics at finite  $T$  and  $\mu_B$  via functional QCD approaches.

In the future:

- Separation of  $\mathcal{L}$  and  $\mathcal{L}^\dagger$ : investigation on  $\varphi_8$  at finite  $\mu_B$ .
- Higher order fluctuations and critical phenomena.
- QCD thermodynamics from inhomogeneous effect/phase structure.

Thanks for your attention!

# Back-up

Why simplifications:

**discrete approach:** difficulties at high density; towards critical end point (CEP);

**continuum approach:** ongoing quests to extract observables from full QCD dynamics.

see e.g. Isserstedt et al., PoS FAIRness 2022 (2023) 024.

Partition function  $Z = Z[G_X]$  in the quantum field theory is a functional of Green functions  $\{G_X\}$ ; QCD involves  $X = \text{quarks, gluons and their coupling (3-pt func.)}$ , etc.

Alternative variables:  $Z = Z[O_X]$ , where  $O$  are the **order parameters**,  
there are connections between the order parameters and the quantum field:

$$O_\chi = \langle \bar{q}q \rangle \leftrightarrow M_q \text{ (mass function),} \quad \text{for chiral phase transition,}$$

$$O_A = \langle A_4 \rangle \leftrightarrow \mathcal{L} \text{ (Polyakov loop),} \quad \text{for deconfinement phase transition.}$$

## Mapping the phase transition line

Modified  $r$  dependence of  $T$ , based on the commonly used linear mapping:

$$\frac{\mu_B}{\mu_B^E} - 1 = -r\omega\rho \cos \alpha_1 - h\omega \cos \alpha_2,$$

$$\frac{T}{T^E} - 1 = f_{\text{PT}}(r) + h\omega \sin \alpha_2.$$

Phase transition line corresponds to  $h = 0$ ; constraint on the map function  $f_{\text{PT}}$ :

$$f_{\text{PT}}(r) = \frac{T_c(\mu_B)}{T^E} - 1 \quad \text{and} \quad \mu_B = \mu_B^E (1 - r\omega\rho \cos \alpha_1),$$

from the transition line:  $\frac{T_c}{T_0} = 1 - \kappa_2 \left( \frac{\mu_B}{T_0} \right)^2 + \kappa_4 \left( \frac{\mu_B}{T_0} \right)^4 + \dots$ ;

up-to-date benchmarks:  $T_0 = 155 \text{ MeV}$ ,  $\kappa_2 \simeq 0.016$ ,  $\kappa_4 \simeq 0$ ;

and estimates:  $\mu_B^E = 600 \text{ MeV}$ ;  $T^E = T_c(\mu_B^E) = 118 \text{ MeV}$ .

WB Collab., PRL (2020), hotQCD Collab., PLB, (2019),

Fu et al., PRD (2019), Gao et al., PLB (2020), Gunkel et al. PRD (2021).

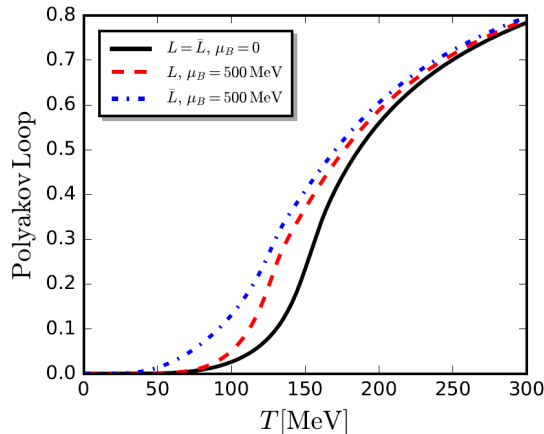
$\varphi_8$  manifests the difference between the conjugated Polyakov loops  $\mathcal{L}$  and  $\mathcal{L}^\dagger$ :

$$\mathcal{L} = \frac{1}{3} \left[ e^{-i\frac{2\pi\varphi_8}{\sqrt{3}}} + 2e^{i\pi\frac{\varphi_8}{\sqrt{3}}} \cos \pi\varphi_3 \right].$$

Typically,  $\varphi_8 = 0$  is the true minimum of the Polyakov potential at  $\mu_B = 0$ .

Preliminary investigation shows that for 2+1-flavour QCD, such difference is small up to  $\mu_B \approx 500$  MeV  $\approx 0.8 \mu_B^{\text{CEP}}$ .

Fu et al., Phys. Rev. D 101: 054032 (2020).

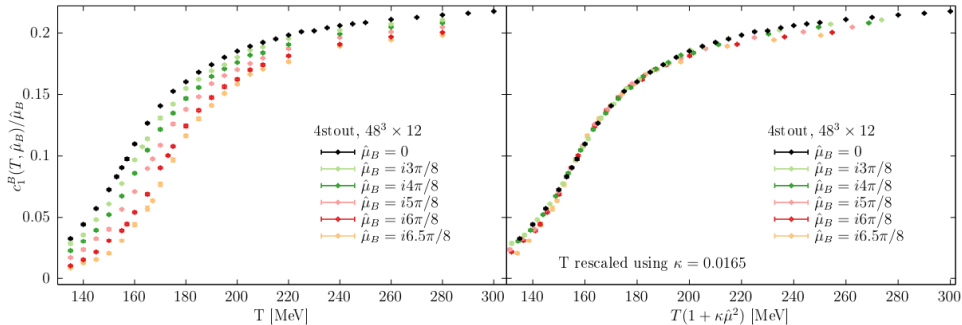


## $T'$ expansion

$$\frac{f(T, \hat{\mu}_B)}{\bar{f}(\hat{\mu}_B)} = \frac{f(T', 0)}{\bar{f}(0)}, \quad \text{Boltzmann limit: } \bar{f}(\hat{\mu}_B) = \lim_{T \rightarrow \infty} f(T, \hat{\mu}_B);$$

$$T' = T + \kappa_2^f(T) \hat{\mu}_B^2 + \kappa_4^f(T) \hat{\mu}_B^4 + \dots.$$

Leading expansion with constant  $\kappa_2^f(T) = \kappa$  already shows remarkably well result;  
see: Borsanyi et.al. (WB-Collab.), PRL 126: 232001 (2021).

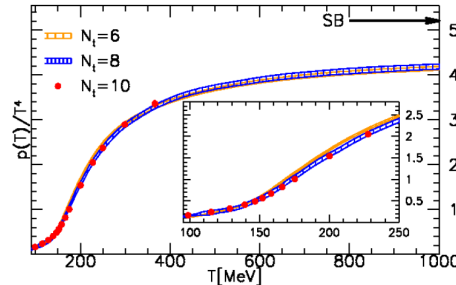
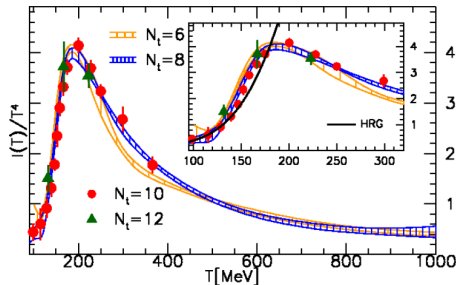


## More on QCD EoS at zero $\mu_B$

Details of the  $T$  dependence - trace anomaly  $I(T) = \epsilon(T) - 3P(T)$ <sup>1,2</sup>:

$$P(T, 0)/T^4 = \int_0^T dT' (I(T')/T'^5).$$

Parametrisation of continuum extrapolated lattice QCD data is available<sup>1</sup>.

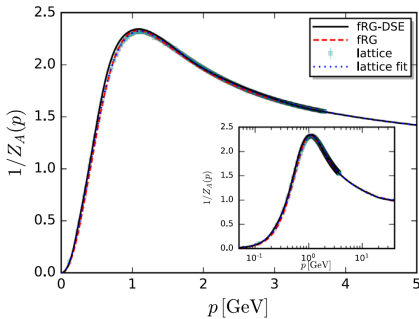


<sup>1</sup> S. Borsanyi, G. Endrodi, Z. Fodor, et al., JHEP 11, 077 (2010)

<sup>2</sup> Bazavov et al. (HotQCD Collab.), Phys. Rev. D 90: 094503 (2014)

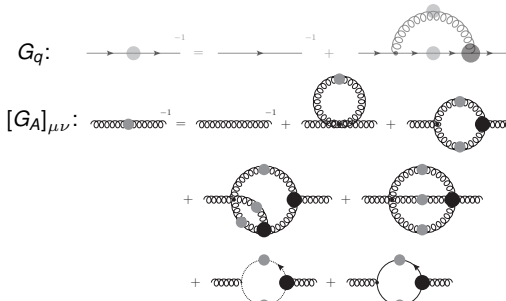
# “Minimal” Dyson-Schwinger equations (DSEs)

- Self-consistent solutions for quark and gluon propagators at finite  $(T, \mu_B)$ ;
- Optimised tensor structures of the quark-gluon vertex;



Vacuum full gluon propagator:

$$p^2[G_A]_{\mu\nu}(p) = 1/Z_A(p^2).$$

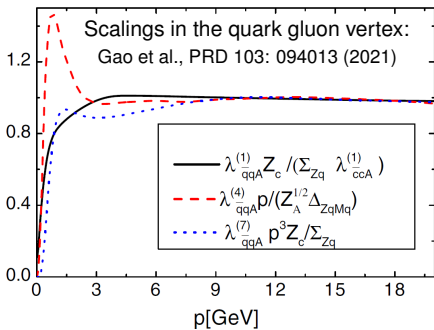


$$[G_A]_{\mu\nu}^{-1}(k) \Big|_{0,0}^{T,\mu_B} = \Pi_{\mu\nu}^{\text{gauge}}(k) \Big|_{0,0}^{T,\mu_B} + \Pi_{\mu\nu}^{\text{qrk}}(k) \Big|_{0,0}^{T,\mu_B}.$$

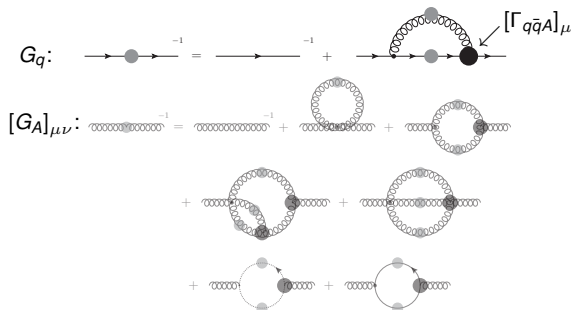
YL et al., Phys. Rev. D 110: 014036 (2024)

# “Minimal” Dyson-Schwinger equations (DSEs)

- Self-consistent solutions for quark and gluon propagators at finite  $(T, \mu_B)$ ;
- Optimised tensor structures of the quark-gluon vertex;



$$[\Gamma_{q\bar{q}A}]_\mu = \lambda_{q\bar{q}A}^{(1)} \gamma_\mu + \lambda_{q\bar{q}A}^{(4)} \sigma_{\mu\nu} k^\nu.$$



$$G_q^{-1}(p) = Z_q(p^2) \left[ i\gamma \cdot p + M_q(p^2) \right].$$

Emphasis on the Pauli term  $\lambda^{(4)}$ : Qin et al. PLB (2013), Williams, EPJA (2015), Cyrol et al. PRD (2018)

# “Minimal” Dyson-Schwinger equations (DSEs)

Benckmarks in: vacuum quark mass function (left);  
finite temperature and density: chiral phase transition line (right).

